Percolation Theory of Creation and Mobilization of Foams in Porous Media

A percolation model of foam mobilization in porous media is developed. This model indicates that there is a minimum pressure gradient or, equivalently, a minimum gas velocity required to initiate mobilization of foam. As a result, for most foam enhanced oil recovery processes, where the surface tension is not low, deep foam penetration depends on propagation of foam formed at a high pressure gradient near the well. Low surface tension makes mobilization of CO_2 foams feasible, however, at pressure gradients found throughout much of the formation in a typical field application. The theory further predicts, and data confirm, that the minimum velocity for foam mobilization during steady flow of liquid and gas decreases as injected liquid volume fraction increases. The theory suggests a better strategy for foam generation: alternate injection of small slugs of liquid and gas.

W. R. Rossen
P. A. Gauglitz
Chevron Oil Field Research Company
La Habra, CA 90633

Introduction

Foams are a promising means to improve reservoir sweep and oil recovery in enhanced oil recovery (EOR) projects involving gas injection (Bailey and Curtis, 1984). However, the existence of a substantial minimum pressure gradient to create and sustain a flowing foam in porous media could limit the successful application of foams to EOR. Maximum gas diversion and sweep improvement requires foam to propagate deep into the formation. Due to the radial nature of flow, a high pressure gradient is available only in the vicinities of the injection and production wells, and the overall pressure drop is limited by the fracture pressure of the formation. Thus, for foam placement deep in the formation, foam must be capable of either generation or propagation at pressure gradients in the vicinity of 23 kPa/m (1 psi/ft) or less.

Experimental observations

The magnitude of the minimum pressure gradient for foam mobilization is controversial. Some have reported foam generation and/or propagation at pressure gradients under 100 kPa/m (5 psi/ft), while others found either no foam or complete plugging instead (see refs. in Rossen, 1990a). The question is complicated by the issue of foam texture, which governs the required pressure gradient, but is seldom known inside the porous medium.

Among those reporting a minimum velocity or pressure gradient specifically for foam *generation* are Falls et al. (1988), who observed a minimum rate of gas invasion required to generate a foam during drainage of a surfactant–liquid-saturated beadpack. Ransohoff and Radke (1988) quantified these rates for low-pressure nitrogen foams as functions of beadpack permeability and injected liquid volume fraction (LVF). In these experiments lamellae were created by "leave-behind" (Ransohoff and Radke, 1988) during drainage of the pack. In other cases (Ali et al., 1985; Friedmann and Jensen, 1986; Isaacs et al., 1988; Sayegh and Girard, 1988; Friedmann et al., 1988) surfactant and gas were injected into a porous medium initially saturated with brine and gas; thus, no leave-behind lamellae were created. Ransohoff and Radke (1988) and Sayegh and Girard (1988) found that the minimum velocity for foam generation rises as beadpack permeability rises. Isaacs et al. (1988), however, found that the minimum velocity for steam-foam generation in Berea sandstone scales roughly as the inverse of permeability. Friedmann et al. (1988) briefly cite the experimental results presented in detail in this paper.

Physical requirements for initial foam mobilization

Until recently (Rossen, 1988b) there has been no theory for the minimum pressure gradient required to initiate foam flow. Most theoretical studies of the mobilization pressure gradient (Slattery, 1979; Falls et al., 1989; Sanchez et al., 1986; Prieditis

Correspondence concerning this paper should be addressed to W. R. Rossen, who is currently with the Petroleum Engineering Department, University of Texas, Austin, TX 78712.

and Flumerfelt, 1988; Rossen, 1990a, b, c) focus on the pressure gradient required to maintain foam flow. These studies fail to account for the multiply connected nature of the pore space. As shown below, the ease of initiating foam flow turns on the existence of multiple alternative gas flow paths not accounted for in these models.

Some definitions help to clarify the issues involved in foam generation: A *lens* is a small slug of liquid occupying the pore throat between two gas-occupied pore bodies. A lens is stable with or without surfactant. If the lens thins down until the surfaces touch and form a film or *lamella,* it breaks unless surfactant stabilizes the film. From the point of view of the gas, both a lens and a lamella block gas flow through the throat.

Creating a flowing foam requires mobilizing the lenses and/or lamellae that block gas flow. This mobilization can happen in three ways, illustrated in Figure 1. Either a lens or a lamella can be displaced from a pore throat, Figures 1a and 1b, if the Δp across the throat is sufficiently large. Once mobilized, lamellae can multiply by lamella division and repeated snap-off at vacated pore throats (Falls et al., 1988; Sanchez et al., 1986; Ransohoff and Radke, 1988). Thus, displacing lenses and lamellae from pore throats initiates processes that refine foam texture even as it initiates the flow of foam itself. Mobilization of lamellae formed by leave-behind, followed by lamella division, was the primary foam-generation mechanism observed by Prieditis (1988) in etched-glass micromodels.

The situation is more complicated if the lens is very thick, as in Figure 1c, or if liquid occupies the pore body across the throat. Gas invades the throat if capillary pressure is high enough. Snap-off of small gas bubbles can occur as gas invades, depending on pore and lens geometry. Ransohoff and Radke (1988) focus on this mechanism; they derive a minimum gas velocity and, by implication, a minimum pressure gradient

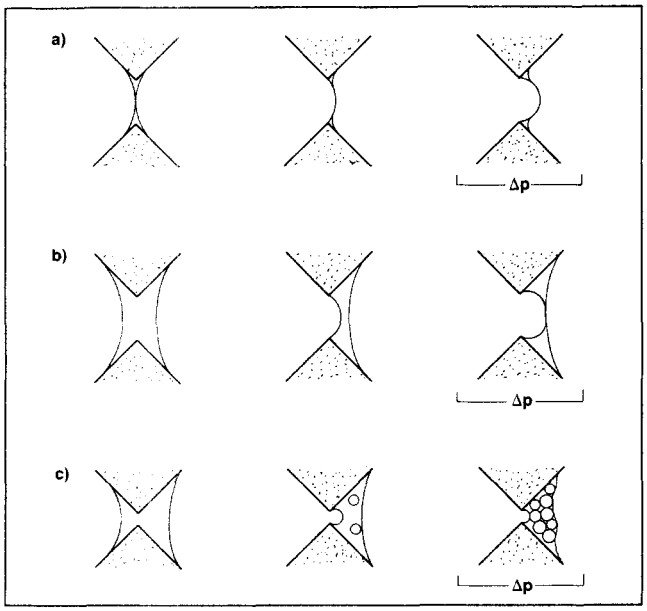

Figure 1. Mobilization of lamellae and lenses.

a. Lamella displacement depends on Δp and, to a lesser extent, on capillary pressure
b. Lens displacement depends on both Δp and capillary pressure
c. Snap-off and subsequent displacement: snap-off depends on capillary pressure, subsequent displacement depends on capillary pressure and Δp

required to form bubbles during gas invasion of a liquid-filled porous medium. However, the minimum velocity or pressure gradient derived depends on core length and the capillary end effect in finite cores; extrapolation to reservoir-length scale is moot. Moreover, their analysis begs the question of mobilizing the lamellae formed, which depends on the pressure difference in the gas phase across the many lamellae created by snap-off. The resistance to gas flow of a series of lamellae is expected to be greater than that required to displace a single lamella or lens (Falls et al., 1989).

Formation of lenses and lamellae

Thus two conditions are necessary for foam mobilization: the existence of lenses or lamellae blocking gas flow and a pressure gradient in the gas phase sufficient to displace them. The existence of a lens depends on the geometry of the pore throat and on capillary pressure. A lens occupies a pore throat if the pore bodies on either side are occupied by gas but the two gas–liquid surfaces do not touch. If the two surfaces do touch and surfactant is present, a leave-behind lamella is formed; if surfactant is absent, the film breaks. Thus, in a brine–gas flood without surfactant, lenses are present in some throats that separate gas-occupied pores; there are no lamellae.

The existence of lamellae depends on fluctuations in capillary pressure after surfactant is introduced. If capillary pressure falls (imbibition), lenses can form in pore throats by snap-off (Roof, 1970; Falls et al., 1988); these lenses may then drain to lamellae as capillary pressure rises again. During a rise in capillary pressure (drainage), lamellae can form by leave-behind and snap-off as gas invades additional pore bodies (Ransohoff and Radke, 1988).

If surfactant solution replaces brine in a brine–gas flood, with no change in saturation, however, and there are no macroscopic variations in pore properties in the medium (Falls et al., 1988), then there are no lamellae; only lenses block the flow of gas and provide sites for initial creation and mobilization of foam.

Mobilization of lenses and lamellae

This paper addresses the minimum pressure gradient required to initiate foam flow, that is, to displace the lenses and lamellae in Figure 1. We assume that the positions of lenses and lamellae can be treated statistically as random and uncorrelated on the pore network. More precisely, at a given capillary pressure, the positions of these lenses and lamellae are a deterministic function of pore geometry and capillary pressure, but pores with the appropriate geometries are assumed to be randomly distributed on the pore network. Our theory applies to mobilization of lenses present in steady gas–liquid flow and also to mobilization of lenses and lamellae created by snap-off during imbibition in a WAG (alternating water–gas) process. It does not quantitatively describe mobilization of lamellae formed by leave-behind and snap-off during drainage in a WAG, but we make some conjectures in the Appendix about mobilization of foams formed during drainage. The minimum mobilization pressure gradient of a preformed foam is covered by our companion papers (Rossen, 1990a, b, c). A brief report of some of this work has been given previously (Rossen, 1988b).

For each lens or lamella, there is a minimum pressure drop across it required to displace it from the pore throat. This Δp is a function of the surface tension between liquid and gas, the geometry of the pore throat, and capillary pressure. For a

lamella, or a lens that thins to a lamella as it is displaced,

$$(\triangle p)^{max} = \frac{4\gamma}{\bar{r}_{min}} \tag{1}$$

where $(\triangle p)^{max}$ is the maximum pressure drop across the lens or lamella as it is displaced from the throat, that is, the minimum $\triangle p$ required to displace it completely; γ is surface tension; and $\bar{r}_{min}$ is the minimum value of $\bar{r} \equiv 2/(1/r_1 + 1/r_2)$ during the displacement, with r_1 and r_2 the principal radii of curvature of the lamella (Bikerman, 1973). At low capillary pressure, the lens may not drain to a lamella before it reaches the position of maximum $\triangle p$, and the relation for $(\triangle p)^{max}$ is more complex.

In general, $\bar{r}_{min}$ is larger than the throat radius r_t. Mast (1972) gives formulas for $\bar{r}_{min}$ for conical and toroidal pores in the limit $p_c \rightarrow \infty$, for which the lamella intersects the pore wall at an angle of 90°. Rossen (1988b) and Prieditis (1988) give values for lower capillary pressure. $(\triangle p)^{max}$ depends on both the size and shape of the pore throat.

If the pressure drop at the pore throat, $\triangle p$, is less than $(\triangle p)^{max}$ for all blocked pore throats, then all of the lenses and lamellae are stranded. In this case the resistance to gas flow depends on the fraction of the pore throats that have been blocked. If relatively few are blocked, gas flow continues through the unblocked pores; the resistance to gas flow in this case is moderate at best. For instance, continuous gas foams with stationary lamellae formed during drainage give measured resistance factors of typically 5–20 (Friedmann et al., 1988; Huh and Handy, 1989; Ransohoff and Radke, 1988; Sanchez and Hazlett, 1989), although values of 50–100 have been reported (Prieditis, 1988). Generating a more effective foam from a continuous gas foam requires mobilizing these lamellae so that they can multiply by lamella division and by repeated snap-off at the vacated pore throats.

On the other hand, if nearly all pore throats are blocked by snap-off during imbibition, the gas phase becomes discontinuous. If the pressure gradient is insufficient to mobilize the blocking lamellae, the flow of gas ceases and the formation is plugged. The distinction between continuous and discontinuous gas regimes is crucial to the mobilization of lenses and lamellae and subsequent foam generation by lamella division and snap-off.

We quantify this distinction and delineate the conditions for foam mobilization using percolation theory. In the next two sections, we describe our theory and derive conditions for foam mobilization. Next, we compare the predictions of this theory to experimental data for the onset of foam moblization in sandstone cores. Finally, we further discuss two implications of these results: an improved injection strategy for foam generation, and the effect of permeability on foam mobilization.

Theory: Continuous Gas

$\triangle p$ across stagnant pore clusters

In a porous medium, the gas phase comprises three fractions:

1. Trapped gas, completely surrounded by liquid-occupied pores or by lenses or lamellae.
2. The backbone fraction, through which gas can flow.
3. The dead-end fraction, only singly connected to the backbone fraction and, therefore, unable to support flow.

We focus here on the subset of pore clusters or pathways in the dead-end fraction that would join the backbone fraction, except that the path is blocked at a single pore throat.

Because the gas is stagnant across this path, the pressure drop across the blocked throat is that between the two points where the path meets the backbone. We define L as the projection of the length between these points in the direction of flow, and approximate the corresponding pressure drop as the product of this distance and the macroscopic pressure gradient ∇p:

$$\triangle p \simeq \nabla p\, L$$

$$(\nabla p)^{min} \simeq (\triangle p)^{max}/L \tag{2}$$

where $(\nabla p)^{min}$ is the minimum pressure gradient required to displace the lamella. We further define n as the number of pores along the pathway that is blocked by the lens or lamella and $\bar{n}$ as the average taken over all such pathways in the pore network. Because the pathways may be tortuous and contain internal loops, for a given pathway it is possible for n to be large while L is relatively small.

Recent work shows that at the threshold between continuous and discontinous gas regimes, the pressure gradient is far from uniform and Eq. 2 is in error (Duxbury et al., 1986, 1987; de Arcangelis et al., 1986; Kahng et al., 1987). It is not yet known how close to this threshold Eq. 2 applies with reasonable accuracy. We discuss this further in the Appendix.

Percolation theory of cluster size

Percolation theory (Larson et al., 1977, 1981a, b; Larson and Morrow, 1981; Stauffer, 1985) gives a means to estimate $\bar{n}$ and L, and, thereby, the pressure gradient at which lamellae are displaced from pore throats. We approximate the interconnected pore network of the porous medium with a network of bonds of as yet unspecified topology (interconnectedness). Nodes (or sites) in the network represent pores, and the bonds connecting them, pore throats. Missing nodes represent pores occupied by water and the removal of additional bonds represents blockage of pore throats by snap-off. Conductivity across the network corresponds to gas permeability, and the potential drop across a missing bond represents the $\triangle p$ across a blocked pore throat, which is the quantity of interest.

The physical processes to be modeled are gas invasion of the liquid-filled, liquid-wet porous medium (no surfactant) at a specified fractional flow, followed by introduction of surfactant into the liquid phase and, possibly, subsequent imbibition and snap-off of a fraction of the gas-occupied pore throats. Rigorous modeling of these processes on even a simplified lattice would be complex, as discussed in the Appendix. Instead we treat both processes as bond percolation problems: we assume the relative permeabilities are governed by occupation of and flow through pore throats. Specifically we make the following assumptions:

1. Only water and gas are present and saturations (occupation of nodes) do not change during subsequent imbibition and snap-off.
2. Each bond has the same conductivity. We discuss the effect of this assumption in the Appendix. Nodes offer no resistance to flow.
3. After initial drainage, snap-off during imbibition occurs at randomly selected pore throats. We also discuss the effects of this assumption in the Appendix.
4. All lenses and lamellae that, by themselves, block dead-end clusters connected to the backbone are free to take the position in the throat where $\triangle p$ is the maximum value, $(\triangle p)^{max}$.

5. As stated above, we approximate the Δp across a lens or lamella according to Eq. 2.

We make no assumptions about the volumes of individual pores (nodes). Therefore, though for convenience we refer to the fraction of pore throats occupied by gas as its saturation, it does not equal the volumetric saturation in the porous medium.

Percolation theory provides the quantities of interest for networks of various topologies. A fraction of bonds f is randomly selected; these are assigned conductivity 1 and the remaining bonds conductivity 0. As a function of f, theory provides tabulations or analytical formulas for

$G(f)$ = conductivity, normalized so $G(1) = 1$
$B(f)$ = backbone fraction: fraction of bonds conducting flow
$F(f)$ = percolation fraction: sum of backbone and dead-end fractions of bonds.

The percolation threshold, f_c, is the value of f at which clusters of bonds link up to form an infinite, though tortuous, network. It is, therefore, the value at which G, B, and F become nonzero, and is a function only of network topology. (Here we have substituted f, f_c, and F for the usual symbols p, p_c, and P to avoid confusion with pressure and pressure gradient.)

The relevance of $G(f)$, $B(f)$, and $F(f)$ to foam mobilization is as follows. When gas invades a brine-saturated porous medium, f represents the fraction of pore throats large enough to be entered at the prevailing capillary pressure. $F(f) \leq f$ represents the fraction of throats actually invaded by gas. Gas occupies enough throats to establish the conductivity, $G(f)$, required for its fractional flow (gas/liquid flow ratio, set externally). We denote the value of f attained at steady state, before surfactant is introduced, f^0; the actual gas saturation at this stage is $F(f^0)$.

During drainage the capillary pressure condition for gas invasion of a liquid-filled pore is that the capillary pressure exceed the capillary entry pressure for at least one throat accessible to the gas phase. Once the pore is entered through one throat, lenses in throats separating it from other gas-filled pores may break at lower capillary pressure than the capillary entry pressures of these throats. Here, for simplicity we assume, as have others applying percolation theory to relative permeabilities (Heiba et al., 1982, 1984), that all bonds in the fraction $(1 - f)$ are blocked to gas flow.

Next, surfactant is introduced into the liquid. If there is subsequent imbibition, snap-off can reduce the value of f. The fraction of initially gas-occupied and accessible throats now blocked, f_{sn}, is

$$f_{sn} = \frac{F(f^0) - [f/f^0]\,F(f^0)}{F(f^0)} = (f^0 - f)/f^0 \qquad (3)$$

Though snap-off reduces the fraction of gas-occupied throats, it does not affect the occupation of pore bodies. Therefore, the fraction of gas now trapped, F_{tr}, is the difference between the fraction initially occupied and that still accessible:

$$F_{tr} = \frac{F(f^0) - F(f)}{F(f^0)} \qquad (4)$$

Equation 4 applies strictly only to the Bethe tree, an idealized network in which there is only one path between any two points (Larson and Davis, 1982). For other, more realistic networks, accounting for trapped gas clusters would be more complex.

One can determine $\bar{n}$, the average number of pores in a gas flow channel blocked by a single pore throat, for any lattice if $B(f)$ is known (Rossen, 1988a):

$$\bar{n} = f\frac{d\ln B}{d\ln f} \qquad (5)$$

Near the percolation threshold

$$\lim_{f\to f_c} \bar{n} = f_c\gamma_B(f - f_c)^{-1} \qquad (6)$$

with γ_B the exponent for the scaling law for B near f_c (Kirkpatrick, 1978; Mohanty et al., 1982). For a Bethe tree of any coordination number, $\gamma_B = 2$ (Larson and Davis, 1982), and, for all three-dimensional lattices, $\gamma_B \simeq 1.11$ (Herrmann and Stanley, 1984). With Eq. 6, $\bar{n}$ can be determined near f_c for the wide variety of lattices for which f_c and γ_B are known: some of these are listed in Table 1. Further from f_c, $\bar{n}$ is given by Eq. 5.

Relating average cluster size to Δp

For any value of f, there is a distribution of values of n for the various missing bonds that, if opened, would contribute to the backbone fraction. In general it is the lamellae blocking the largest clusters that have the largest Δp, and thus these lamellae are mobilized first. Therefore, we focus on the tail end of the frequency distribution of n represented by $\bar{n} > 3$. (If the frequency distribution of n decayed exponentially with cluster size, for instance, one could show that $n > 3\bar{n}$ would represent the largest 5% of the blocked clusters present.) Further, clusters of pores will vary from straight to tortuous. We focus on straight clusters because, again, these longest clusters are most likely to mobilize lamellae first. For pores in a straight line, the clusters of size $3\bar{n}$ have length $3\bar{n}\,\ell$, where ℓ is the length of a single pore. The projection of this cluster in the direction of flow is $3\bar{n}\,\ell\cos\theta$, where θ is the angle between the cluster and flow directions. We assume that the probability distribution for the cluster direction is distributed uniformly on the surface of a unit sphere. Multiplying the projected length by the differential surface area element, integrating over all directions θ and Ψ, and scaling by

Table 1. Percolation Threshold and Backbone Exponent for Various Networks*

Network	γ_B	f_c for Bond Percolation
Three-dimensional	1.11 ± 0.05**	
Simple cubic		0.2492
Body-centered cubic		0.1785
BCC2***		0.0991†
Face-centered cubic		0.119
Voronoi		0.08922†
Bethe Tree‡	2	$1/(z-1)$

*Estimates from Stauffer (1985) except as noted
**Herrmann and Stanley (1984); see also Herrmann et al. (1984), Jerauld et al. (1984), Sarychev et al. (1985), Kirkpatrick (1978)
***Body-centered cubic network with bonding between second-nearest neighbors
†Jerauld et al. (1984)
‡Stinchcombe (1973, 1974)

the surface area of the sphere gives an estimate for the average cluster length in the direction of flow.

$$L \simeq 3\bar{n}\ell \left\{ \frac{1}{2\pi} \int_0^{\pi/2} \int_0^{2\pi} \cos\Theta \sin\Theta \, d\Theta \, d\Psi \right\}$$

$$L \simeq \frac{3}{2} \bar{n} \ell \tag{7}$$

Together, Eqs. 2, 6, and 7 indicate that, near the percolation threshold, the minimum mobilization pressure gradient varies linearly with f.

By ignoring the tortuosity of clusters in Eq. 7, we overestimate their characteristic length L and, by implication, underestimate $(\nabla p)^{min}$, Eq. 2. Although the exact relation between L and $\bar{n}$ on three-dimensional lattices is unknown, tortuosity can be considered by treating clusters as random walks of $3\bar{n}$ steps. In this case, the root mean square length of the path is $(3\bar{n})^{1/2}\ell$ (Flory, 1953), and the projection in the direction of flow is $L \sim (3\bar{n})^{1/2}\ell/2$. This approximation applies when the clusters are very large near the percolation threshold. However, as discussed in the Appendix, recent studies show that Eq. 2 becomes inaccurate near the percolation threshold. Further, when the clusters are small or intermediate in size, this approximation underestimates L. Because we focus on the largest and longest clusters, we will primarily use the approximation given by Eq. 7.

Equations 2, 5, and 7 give $(\nabla p)^{min}$, the minimum pressure gradient required to displace the lenses or lamellae that block gas flow, that is, to initiate flow of foam. At the onset of foam mobilization, Darcy's law (Collins, 1961) relates $(\nabla p)^{min}$ to the minimum gas velocity for mobilization, v_g^{min}:

$$v_g^{min} = \frac{kG(f)}{\phi \mu_g} (\nabla p)^{min} \tag{8}$$

where k is absolute permeability, $G(f)$ represents relative permeability to gas, ϕ is porosity, μ_g is gas viscosity, and v_g^{min} is the critical gas frontal advance rate, that is, volumetric injection rate per unit area divided by porosity.

Parameter values used

For detailed calculations we select the Bethe tree network, for which analytical formulas are available for f_c, B, and F (Larson and Davis, 1982). We use a coordination number (number of bonds at each node) $z = 5$. This network (with more realistic distributions of pore sizes than used here) has modeled two- and three-phase relative permeabilities accurately (Heiba et al., 1982, 1984). For conductivity G, we combine the quadratic approximation valid as f approaches f_c with the five-term expansion valid for f far from f_c (Stinchcombe, 1973, 1974; Mohanty et al., 1982).

The model requires a description of core and pore properties as well as network topology, Eqs. 1, 5, 7, and 8. We use, as representative values, a pore length ℓ of 150 μm and a relatively large pore throat radius r_t of 50 μm. For surface tension γ we use two values: 30 and 5 mN/m (dyne/cm). The higher value applies to nitrogen with a variety of foamers and has been used in a number of theoretical studies (Falls et al., 1988; Lau and O'Brien, 1988; Prieditis and Flumerfelt, 1988; Huang et al., 1986; Sanchez et al., 1986; Hirasaki and Lawson, 1985). The lower value applies to foams of compressed CO_2 (Wellington and Vinegar, 1987). We assume $k = 0.75$ μm^2, $\phi = 0.24$, and $\mu_g = 2 \times 10^{-5}$ Pa · s (0.02 cp). Finally, for $\bar{r}_{min}$, we take a somewhat large estimate of $4r_t$ (Mast, 1972), independent of capillary pressure. The generous estimates of r_t and $\bar{r}_{min}$ give lower-bound values for $(\triangle p)^{max}$, 100 and 600 Pa (0.015 and 0.087 psi) for CO_2 and other foams, respectively, Eq. 1. Moreover, our choice to ignore cluster tortuosity, Eq. 7, tends to inflate L. Therefore, we expect that our estimates of $(\nabla p)^{min}$, if anything, underestimate the true values. One can now calculate conductivity (gas and liquid relative permeabilities), $\bar{n}$, v_g^{min}, and other quantities of interest.

Theory: Discontinuous Gas Foams

In the case of a discontinuous gas foam, gas invades to an initial $f^0 > f_c$, but then, during imbibition, snap-off reduces f to a value below f_c. All gas is trapped gas unless the blocking lamellae can be mobilized.

Gas flow begins along the pathway blocked by the fewest lamellae:

$$(\nabla p)^{min} = min\,\{(\triangle p)^{max}/L'\} \tag{9}$$

where L' is the average distance in the direction of flow between lamellae along this path, and the minimization is carried out over all possible pathways. We approximate L' with the following intuitive arguments.

Presumably this pathway samples the largest clusters of gas-filled pores so as to minimize the number of blocking lamellae. In order to form the infinite pathway required for flow, however, the clusters it samples must occupy at least the percolation fraction, f_c, of the pore space. Here, instead of the Bethe tree f_c, we use the lower threshold 0.1, which is a conservative estimate of f_c for three-dimensional lattices, Table 1. Thus, for given values of f and f^0, the path samples the fraction $(0.10/f^0)$ of the gas-occupied pore space containing the largest clusters. If the cluster size distribution function is a decreasing exponential function of cluster size, this means the path samples clusters of size at least $\ell n(f^0/0.1)$ times the mean cluster size, and the average cluster in this fraction has size $1 + \ell n(f^0/0.1)$ times the mean for the entire population. This factor lies below 3 for the values of f^0 we derive below, so for simplicity we assume the pathway samples clusters of size three times the mean for the given value of f. If instead of 0.1 we chose 0.25, the percolation threshold for the Bethe tree under study, the average cluster would be less than twice the mean and $(\nabla p)^{min}$ would be 50% higher than calculated below.

The mean cluster size for bond percolation on a Bethe tree for $f < f_c$ is (Fisher and Essam, 1961)

$$S(f) = \frac{1 + (z-1)f}{1 - (z-1)f} \tag{10}$$

We ignore tortuosity in the clusters and pathway and assume

$$L' = 3S(f)\ell$$

$$(\nabla p)^{min} \simeq (\triangle p)^{max}/[3S(f)\ell] \tag{11}$$

We expect that Eq. 11 underestimates $(\nabla p)^{min}$ both due to the generous estimate of cluster size and the exclusion of tortuosity.

For three-dimensional lattices the average length spanned by a cluster increases near f_c as $(f - f_c)^{-0.88}$ (Essam, 1980; Coniglio, 1982), which is not much different than $(f - f_c)^{-1}$, as implied by Eqs. 10 and 11.

Results of Theory: Continuous Gas Foam

Drainage

The gas saturation before surfactant is introduced is crucial to foam mobilization, with or without subsequent imbibition. We examine three cases. In the first, injected liquid volume fraction (*LVF*) is 10% and the ratio of gas to water viscosity is 1/50, as it is for nitrogen and water at room temperature (Perry and Chilton, 1973). The fractional-flow equation for horizontal flow without capillary pressure gradients (Collins, 1961) relates *LVF* to the relative permeabilities to water, k_{rw}, and gas, k_{rg}, which we approximate as $G(f^0)$ and $G[1 - F(f^0)]$ (Heiba et al., 1982, 1984). Solving this equation gives $f^0 = 0.356$; $F(f^0 = 0.356) = 0.312$. This estimate of f^0 also corresponds roughly to a CO_2 flood in which the ratio of viscosities is 1/10 and the fractional flow of CO_2 is 0.65. (Lower fractional flows of CO_2 would give still lower values of f^0, closer to the percolation threshold $f_c = 0.25$.)

Our second case has $LVF = 0.1$ and a ratio of viscosities of 1/10 that applies to a CO_2 flood or to a nitrogen–water flood at 420 K (300°F). We estimate for this case $f^0 = 0.513$ and $F(f^0) = 0.510$.

The third case has a lower *LVF*, 0.02, more typical of steamflood field applications, and a ratio of viscosities of 1/10. We estimate for this case $f^0 \simeq F(f^0) = 0.650$.

Imbibition

Given an initial condition defined by f^0, one can determine the ease of mobilizing foam in steady flow or after subsequent imbibition. We focus first, however, on the change in flow properties upon imbibition at velocities insufficient to mobilize foam. During imbibition snap-off proceeds to an extent governed by pore geometry and capillary pressure.

Figure 2 shows how f relates to the fraction of previously gas-occupied throats blocked by snap-off, f_{sn}, Eq. 3. If initial gas saturation is relatively high, illustrated by $f^0 = 0.513$ or 0.650, over half of the gas-occupied pore throats must be blocked by snap-off to approach the percolation threshold, where the gas phase becomes discontinuous. But if initial gas saturation is lower ($f^0 = 0.356$), as expected when the gas fractional flow and the gas/liquid viscosity ratio are low, then snap-off of only about 30% of the gas-occupied throats brings the gas phase to the percolation threshold.

Figure 3 shows that as snap-off blocks more pore throats (i.e., f decreases) during imbibition, resistance to gas flow increases. Here we define the resistance factor, *RF*, as the ratio of the conductivity of the gas-occupied network before snap-off to the conductivity of the network at the same saturation after snap-off:

$$RF \equiv G(f^0)/G(f) \tag{12}$$

In a porous medium gas saturation (and f) would rise to maintain its fractional flow as snap-off reduces gas relative permeability, and measured gas flow resistance would be lower than that shown here. The curve for $f^0 = 1$, Figure 3, corresponds to an initially fully gas-saturated porous medium. In that case *RF* corresponds to the inverse of gas relative permeability.

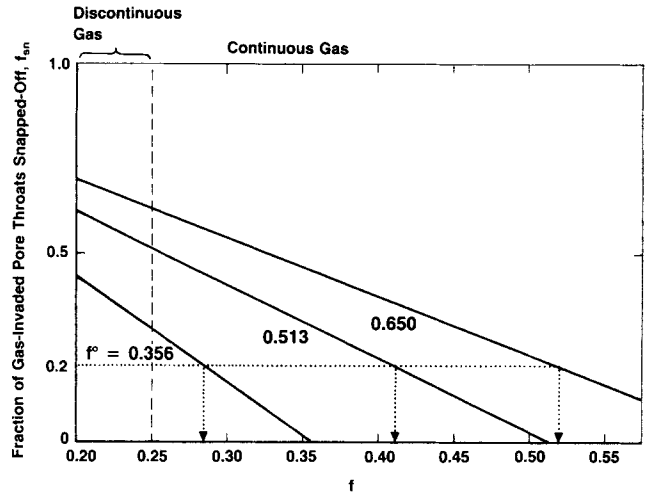

Figure 2. Fraction of gas-occupied pore throats blocked by snap-off, f_{sn}, corresponding to a given value of *f*.

· · · · · *f* for 20% of throats snapped off
– – – – –Percolation threshold

Because *RF* rises so sharply at the percolation threshold $f_c = 0.25$, Figure 3, fewer throats need be blocked to achieve a substantial *RF* if the initial saturation is lower. This is because, at low saturation, the gas-occupied pore network is already tortuous and inefficient before snap-off begins. For instance,

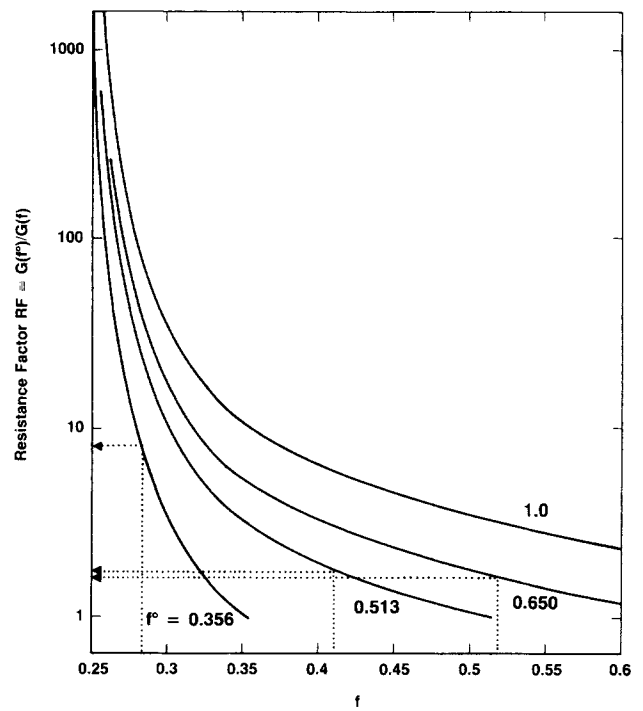

Figure 3. Resistance factor *RF* for continuous gas as a function of initial (f^0) and final values of *f*.

· · · · · *RF* for 20% of throats snapped off, cf. Figure 2

blocking 20% of gas-occupied pore throats ($f_{sn} = 0.2$) gives resistance factors of 7.9, 1.8, and 1.6 for $f^0 = 0.356$, 0.513, and 0.650, shown by dotted lines in Figures 2 and 3

Figure 4 shows the fraction of gas present that is trapped as a function of f for the three initial gas saturations. For f below the percolation threshold, all gas is trapped unless lenses and lamellae are mobilized.

These results assume that lenses and lamallae formed during imbibition are stable. If these lenses and lamellae thin and break upon subsequent drainage, for instance, then f reflects the fraction of throats still blocked after drainage.

Foam mobilization

The righthand side of Figure 5 ($f > f_c = 0.25$) shows $\bar{n}$, the average size of the clusters of pores blocked at a single pore throat, and $(\nabla p)^{min}$, the pressure gradient required to mobilize the lenses and lamellae blocking the largest of these clusters, as functions of f (Eqs. 2, 5, and 7). These curves apply whether $f = f^0$ as in steady flow or f has been reduced by imbibition. Figure 5 assumes $\gamma = 30$ mN/m (dyne/cm); for CO_2 foams, lower surface tension would reduce the values of $(\nabla p)^{min}$ from Figure 5 by a factor of 6. For most foams, Figure 5 shows that lenses and lamellae can be mobilized by pressure gradients below 230 kPa/m (10 psi/ft) only if f is approximately 0.29 or below. Figure 2 shows that for high initial gas saturations ($f^0 = 0.513$ or 0.650), this can happen only if about half the pore throats are blocked by snap-off during imbibition. For low initial gas saturations ($f^0 = 0.356$), mobilizing the lamellae at 10 psi/ft requires that only about 15 to 20% of the throats be blocked. For all three saturations, mobilization cannot occur at under 230 kPa/m (10 psi/ft) in steady flow; at least some additional throats must be blocked during imbibition. In fact, for most foams mobilization in steady flow at 2 psi/ft would require $f = f^0 < 0.26$, Figure 5, or if $\mu_w/\mu_g = 50$, $LVF > 0.94$.

For CO_2 foams, however, the implications of Figure 5 are markedly different due to sixfold lower surface tension. CO_2 foams can be mobilized at 10 psi/ft for $f < 0.50$ and at 2 psi/ft for $f < 0.30$. In other words, CO_2 foams can be mobilized at roughly 10 psi/ft in steady flow ($f = f^0$) in two of the three cases we have considered ($f^0 = 0.356$ and 0.513), and at 2 psi/ft for $f^0 = 0.356$.

Percolation theory not only relates $(\nabla p)^{min}$ to f but relates f to relative permeabilities and, thereby, to flow velocities and

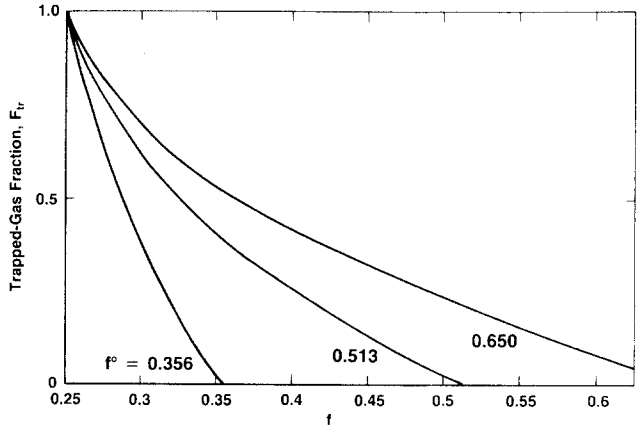

Figure 4. Trapped gas fraction F_{tr} as a function of f.

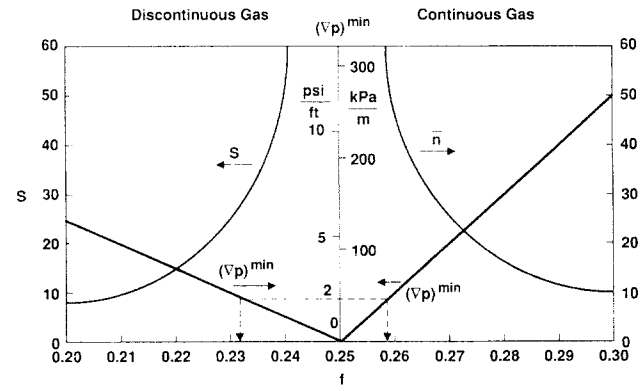

Figure 5. Cluster sizes $\bar{n}$ and S and minimum pressure gradient $(\nabla p)^{min}$ required to mobilize discontinuous and continuous gas foams as functions of f.

. . . f range within which foam is mobilized at 45 kPa/m (2 psi/ft). $(\nabla Vp)^{min}$ for CO_2 foams is 1/6 values given here

injected LVF. Figure 6 shows how $(\nabla p)^{min}$ varies with LVF in steady flow. The pressure gradient required to mobilize foam is greatest when LVF is low, that is, for steady, "dry" liquid–gas streams.

Figure 7 shows how the minimum gas velocity for foam mobilization in steady flow, v_g^{min}, Eq. 8, depends on LVF for a range of values of μ_g/μ_w, with μ_g fixed at $2 \cdot 10^{-5}$ $Pa \cdot s$ (0.02 cp). In all cases foam is mobilized at a lower velocity when LVF is high (wet foam) than when LVF is low (dry foam). Surprisingly, the absolute value of v_g^{min} increases with increasing μ_g/μ_w, because we have fixed μ_g in Figure 7; as μ_g/μ_w increases, μ_w decreases, water saturation decreases, and there are fewer

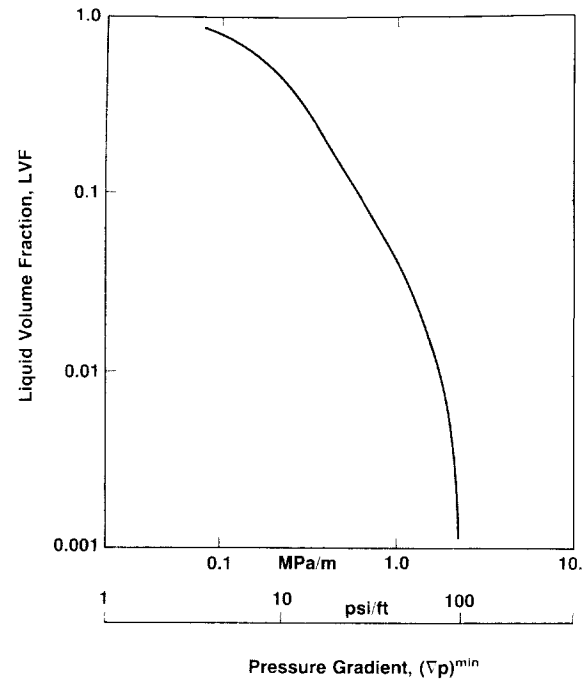

Figure 6. Minimum pressure gradient $(\nabla p)^{min}$ required to mobilize foam in steady flow as a function of injected volume fraction, LVF.

$(\nabla p)^{min}$ for CO_2 foams is 1/6 values shown here

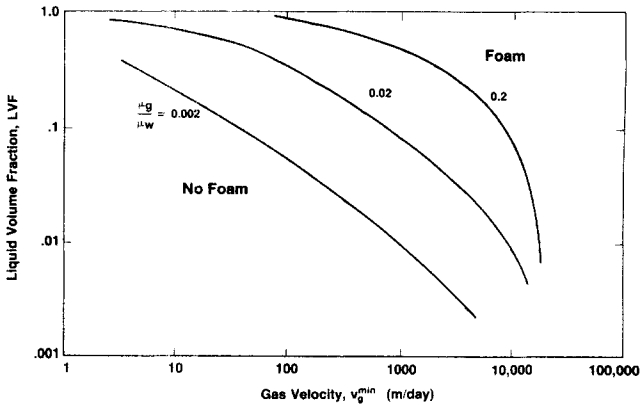

Figure 7. Minimum gas velocity for foam mobilization v_g^{min} as a function of injected liquid volume fraction *LVF* and viscosity ratio.

v_g^{min} for CO_2 foams is 1/30 values shown here

blocked pore throats available for mobilization. For fixed μ_g/μ_w, v_g^{min} in Figure 7 scales proportionally to $1/\mu_g$.

Both Figures 6 and 7 assume $\gamma = 30$ mN/m (dyne/cm). Thus the values of $(\nabla p)^{min}$ and v_g^{min} for CO_2 foams are, respectively, 6 times lower than in Figure 1b, and 30 times lower than in Figure 7 due to the higher viscosity of CO_2 than the value assumed there. Mobilization of CO_2 foams in steady flow at low ∇p is feasible, if injected *LVF* is relatively high (a few tens of percent), as is often the case.

As noted in the Introduction, $(\nabla p)^{min}$ depends on the pore-geometry parameters that govern $(\triangle p)^{max}$ (Mast, 1972). For a fixed pore length and shape, $(\triangle p)^{max}$ and $(\nabla p)^{min}$ scale inversely as r_t, Eq. 1. Other parameters in the theory include liquid–gas surface tension γ, Eq. 1, pore length ℓ, Eq. 7 or 11, injected *LVF*, and the ratio of gas to liquid viscosities, μ_g/μ_w.

Theory Results: Discontinuous Gas

If f falls below f_c, all gas is trapped and *RF* is infinite unless the blocking lamellae can be mobilized according to Eq. 11.

The mean cluster size below the percolation threshold and the computed minimum mobilization pressure gradient are shown on the left side of Figure 5 ($f < f_c = 0.25$). For most foams, Figure 5 indicates that there is a narrow range of f in which an effective flowing foam can be created at field pressure gradients of 45 kPa/m (2 psi/ft): from about $f = 0.234$ to 0.258. If f is above this range, a stranded, ineffective foam results. If f is below this range, gas flow stops and the formation is plugged at the given pressure gradient. For most foams only near the well is ∇p high enough to mobilize foams.

The practical implication of this result is that, except for CO_2 foams, the initial mobilization of foams can be expected only near the wellbore. Subsequent deep foam penetration is possible if the foam first formed at the well can propagate throughout the formation. If, for some reason, the foam mobilized at the well fails to propagate, then gas-flow resistance deep in the formation would be limited to that attainable by snap-off and leave-behind alone.

As before, the conclusions are markedly different for CO_2 foams. Lower surface tension means foam can be mobilized at 20–45 kPa/m (2 psi/ft) for f between 0.165 and 0.30, and at 220 kPa/m (10 psi/ft) for all values of f below 0.50. Foam mobilization at relatively low ∇p appears feasible for CO_2 foams injected with a significant *LVF*.

Experimental Method

Theory predicts a minimum pressure gradient—Eqs. 1, 2, 5, and 7—or velocity, Eq. 8, necessary to mobilize lamellae or lenses from pore throats. Experiments in linear cores were designed to measure the minimum velocity for foam mobilization in steady flow and to quantify how the minimum velocity depends on the injected *LVF*.

Foam mobilization rapidly refines foam texture and reduces gas mobility once mobilization begins. Therefore, the mark of foam mobilization in these experiments is a sudden, sharp drop in gas mobility. The gas relative mobility, k_{rg}/μ_g, is defined by Darcy's law

$$k_{rg}/\mu_g = v_g\phi/[(\triangle p_t/Z)k] \tag{13}$$

where, as before, v_g is gas frontal advance rate, that is, volumetric injection rate per unit area divided by porosity ϕ; $\triangle p_t$ is the total pressure drop across the core; Z is core length; and k is core permeability. Note that while relative mobility is defined as the ratio of relative permeability to viscosity, what is measured is v_g and $\triangle p_t$.

In these experiments the initial condition before foam mobilization is steady flow of surfactant solution and gas in the absence of bubbles and leave-behind lamellae. We employed the following flooding sequence in order to ensure this condition. For each experiment a core is saturated with surfactant-free brine, then flooded with nitrogen and brine (drainage) at a constant *LVF* until steady state. This flood is performed at a flow rate below the velocity required for foam mobilization. After achieving steady saturations, the liquid is switched from brine to surfactant solution without changing the gas or liquid flow rates. Injection continues for many pore volumes in order to saturate rock surfaces with surfactant. The flow rates are then increased in steps until the mobility of the gas sharply decreases, signaling foam mobilization.

Apparatus

The apparatus is essentially that in Friedmann et al. (1988), without a foam pregenerator and with a modified method of liquid injection. A Brooks 5850E mass flow controller (Instrument Div., Emerson Electric Co.) regulates nitrogen into the core through the end face at a constant mass rate. Brine or surfactant solution is injected into the core through four 0.8 cm dia. taps located 2.5 cm from the inlet coreface and spaced evenly about the circumference. A single Tracor 951 LC pump drives surfactant solution or brine from cylinders with floating pistons. An automatic valve (Valco Instruments Co.) switches injection from brine to surfactant solution near the core inlet. The line volume between the automatic value and the liquid inlet taps is 2.5 cm.[3] In our experiments the surfactant solution was 1 wt. % active Chevron Chaser SD1000 in 0.1% NaCl brine.

The porous media were Berea sandstone cores, 38 to 58 cm long, of approximately 0.75 μm^2 (750 md) permeability, potted with epoxy in stainless steel tubes. Gas and liquid exit from the core in a single line that enters a liquid-level gauge (Inferno Manufacturing Corp.). Silicone high-vacuum grease (Dow Corning Corp.) coating the inside of the liquid-level gauge breaks the foam, allowing liquid to collect in the gauge and gas

to exit. The gas then flows through a Temco Dome Loaded BP Series (Temco, Inc.) backpressure regulator.

Most experiments employed separate injection lines for gas and liquid, eliminating mixing upstream from the core inlet. Coinjecting through a single line at the coreface sometimes gave a stagnant region of reduced gas mobility within the first few centimeters near the core inlet, even below the critical velocity for foam mobilization. We believe this was due to injecting small slugs of gas (drainage) and liquid (imbibition) at the coreface, generating stranded lenses and lamellae that reduce gas mobility.

Experimental Results

Figure 8 shows the inverse of the gas mobility, Eq. 13, for a foam-generation experiment with an *LVF* of 0.02. After 300 min liquid flow was switched from brine to surfactant solution. The gas frontal advance rate was held constant at 86 m/d for about 900 min, which allowed sufficient time for surfactant to propagate through the core. Gas mobility was nearly unchanged by the switch to injection of surfactant solution, implying that, during this time, virtually no bubbles were formed by snap-off or lamella division and no leave-behind lamellae were formed. The mobility changed slightly when the gas frontal advance rate was increased from 86 to 172 m/d and then to 343 m/d. However, upon increasing the injection rate to 686 m/d, the inverse mobility increased rapidly. This signifies foam mobilization.

Figure 9 plots the results of a number of experiments defining when foam mobilization occurs for a range of gas velocities and *LVF*s. Different symbols distinguish whether or not foam was observed and whether gas and liquid were injected through separate lines or coinjected through a single line. For comparison, Figure 9 also plots the results of Friedmann and Jensen (1986). The experiments with separate injection lines and those of Friedmann and Jensen were at ambient temperture. The coinjection results represent a range of temperatures, but temperature appears to have a minor influence.

The experimental results in Figure 9 confirm that the minimum velocity for generating a flowing foam decreases with

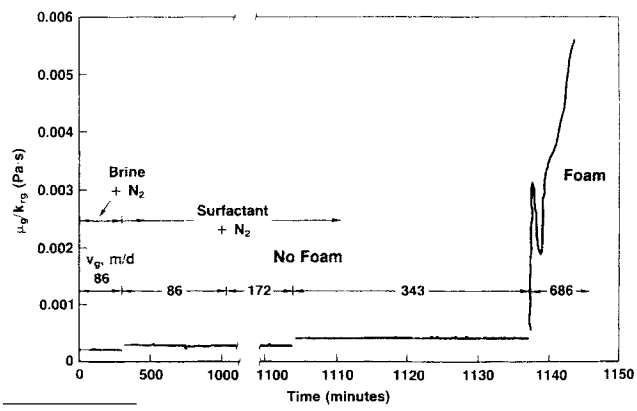

Figure 8. Inverse gas relative mobility μ_g/k_{rg} as a function of time with increasing gas frontal advance rate v_g. Exp. conditions: *LVF* = 0.02; k = 0.68 μm^2; ϕ = 0.27; core length = 38.1 cm; temp. = 22°C

Nitrogen foam is mobilized at 686 m/day

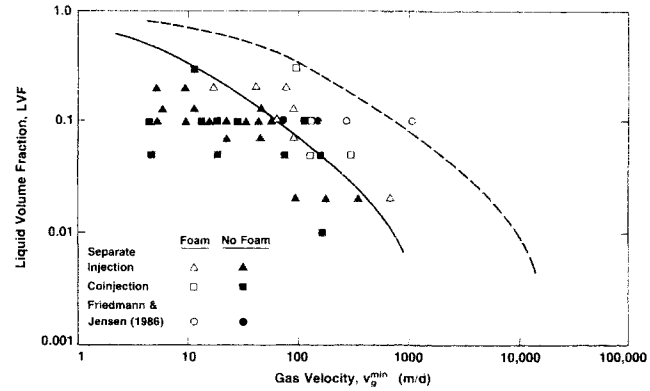

Figure 9. Comparison of theory and data for minimum gas velocity v_g^{min}, for nitrogen foam mobilization as a function of injected *LVF*.

Predictions of theory: ------ using parameters in text; ——— best fit.

increasing *LVF*. Theory predicts this trend quite well, although the predicted minimum velocity is too high. Shifting the theory for v_g^{min}, without changing the shape of the curve, to give the best eye fit demonstrates how well the theory predicts the effect of the *LVF*. The lateral shift of the theory is equivalent to changing any combination of the following: ℓ and the constants in Eq. 7; $(\triangle p)^{max}$, Eq. 2; and the relative and absolute permeabilities, see Eq. 8. No attempt has been made to tune the model to these data.

We do not report $(\nabla p)^{min}$ for these experiments because our measurements had large uncertainty in the low ∇p regime before mobilization. Limited observations, however, suggest a fairly good agreement between measured $(\nabla p)^{min}$ and Figure 6. For instance, in our experiments, $(\nabla p)^{min}$ for *LVF* = 0.1 appeared to be roughly 900 kPa/m (40 psi/ft). In agreement with our limited observations, Baghdikian and Handy (1990) report foam mobilization occurring at about 670 kPa/m (30 psi/ft) for essentially identical experimental conditions: 0.1 m long, 700 μm^2 Berea core; *LVF* = 0.11; Chaser SD1000 surfactant. In contrast to the difference between theory and data for v_g^{min} in Figure 9, our simple theory underestimates $(\nabla p)^{min}$, at 530 kPa/m (24 psi/ft). Evidently, then, the fact that the theoretical prediction is too high in Figure 9 is due to how the model relates v_g^{min} to $(\nabla p)^{min}$, not to the theory of $(\nabla p)^{min}$ itself. More accurate pore size distributions are necessary for quantitative percolation modeling of relative permeabilities (Heiba et al., 1982, 1984). We expect the model to underestimate $(\nabla p)^{min}$ due, for instance, to exclusion of tortuosity from the model for cluster length.

In constrast to the trends in Figure 9, Figures 11 and 12 of Ransohoff and Radke (1988) indicate that for their beadpack of 0.05 cm beads, v_g^{min} decreases slightly with increasing *LVF*. The discrepancy is probably due to formation of leave-behind lamellae in their drainage experiments, which we strove to exclude from ours.

Our experiments demonstrate that a flowing foam can be generated without lamellae being present initially. We believe lenses of wetting liquid were mobilized, leading to lamella division and repeated snap-off at vacated pore throats.

Discussion

Injection strategies

The results in Figure 9 indicate a rule of thumb for effective foam generation by simultaneous injection of liquid and gas: if, under given conditions, little or no foam generation occurs, increasing injection rate and/or *LVF* may give an effective foam.

The importance of snap-off to lamella creation and mobilization suggests, however, that the most effective foam-generation strategy is alternate injection of liquid and gas. In other words, v_g^{min} can be reduced below that for steady flow at the same overall *LVF* by alternating liquid and gas slugs. In this strategy, capillary pressure varies greatly as the slugs pass each location in the rock. During imbibition (liquid slug) lamellae form by snap-off in gas-occupied throats. During drainage (gas slug) lamellae form by leave-behind and snap-off as gas invades liquid-occupied pore bodies (Ransohoff and Radke, 1988). If gas fractional flow falls to zero at a given location during passage of the liquid slug, then the gas phase is at or below the percolation threshold, the optimal condition for lamella mobilization when gas flow resumes. Of course, if f falls below the percolation threshold, then the pressure gradient required to mobilize the gas phase can again become significant, Figure 5. Small alternating slugs can plug a zone entirely (Raza, 1970).

For most foam processes our percolation theory indicates that foam mobilization is enhanced with alternating slugs only if the slugs contact each other in the near wellbore region, where ∇p is high enough to mobilize the lamellae that are formed. Again, a rule of thumb suggests itself: if during injection of the gas slug injectivity rises to nearly the prefoam level, then it is time for another slug of liquid. High injectivity indicates that foam is no longer generated near the well, and if there is no generation near the well, then probably the creation of mobile foam has ceased throughout the formation. Foam previously generated and mobilized near the well could continue to propagate (Rossen, 1990a, b, c), but the nonfoamed, high-mobility gas subsequently injected would tend to finger through and bypass it.

For CO_2 foams, on the other hand, mobilization at low ∇p away from the well may be feasible, It is less crucial that foam generation and mobilization occur in the immediate vicinity of the wellbore.

How $(\nabla p)^{min}$ scales with permeability

Our theory indicates that for a given pore shape and network topology, $(\nabla p)^{min}$ is proportional to $1/(\ell r_t)$, where ℓ is pore length and r_t is throat radius, Eqs. 1, 2, 7, and 11. This proportionality assumes also that, in geometrically similar networks, capillary pressure is scaled so that the fraction of throats blocked by liquid is the same in both media. Such control would be difficult to achieve in practice.

If this condition were met, however, then one could relate $(\nabla p)^{min}$ to the permeability of the medium, k. For instance, for beadpacks, both ℓ and r_t are proportional to bead radius R, and k is proportional to R^2 (Falls et al., 1989). Thus, all else being equal, $(\nabla p)^{min}$ should scale as $1/R^2 \sim 1/k$, and v_g^{min} should be independent of k.

The limited available data for beadpacks and sandpacks differ on this point (Ransohoff and Radke, 1988; Sayegh and Girard, 1988; Isaacs et al., 1988). However, interpreting these data is complicated by the presence of leave-behind lamellae, limited range of data, and steam condensation and evaporation. Further experimental data are required to understand how $(\nabla p)^{min}$ and v_g^{min} depend on permeability and pore shape.

The same relations between $(\nabla p)^{min}$, k, and v_g^{min} should hold for lightly cemented rocks in which pore length and throat radius are proportional to grain size (Wardlaw and Cassan, 1978; Wardlaw, 1979). For more highly cemented and altered rocks, scaling depends on the processes that control r_t, ℓ, and k.

What happens after the first lamella moves

The theory described here predicts the pressure gradient required to mobilize the first lamella (or the first few). As this lamella passes each pore body, it is likely to leave static lamellae in each unblocked pore throat connected to that body by the mechanism of lamella division (Prieditis, 1988). One result of the onset of lamella movement, if lamellae do not break as they move, is a discontinuous gas foam of increasingly finer foam texture. Our experimental data show, for instance, a sharp rise in $\triangle p$ upon mobilization. For this reason it is unlikely that the mobilization pressure gradient approaches zero even at the percolation threshold, f_c. Our theory cannot predict the mobilization pressure gradient once flow begins, however.

The high ∇p required initially to mobilize most foams raises the question: how can foams mobilized by high ∇p near the well stay mobile at low ∇p away from the well?

Flowing bubbles may be longer (up to 60 pores in Falls et al., 1989) than the gas clusters (L in Eq. 7) at the onset of foam mobilization. In addition, two crucial assumptions of the theory for initial mobilization are violated by established, flowing foams: the first violation is that flowing lamellae are not distributed in a random and uncorrelated way in the pore network. The second is that not all flowing lamellae occupy simultaneously the positions of maximum resistance to flow: that is, that $\triangle p = (\triangle p)^{max}$ in Eq. 2. Each of these points assists flowing foams to stay mobile at low ∇p away from the well.

Lamellae are not distributed randomly in flowing foams, especially at low ∇p where foams flow in bubble trains along sinuous paths through regions of trapped gas (Falls et al., 1989; Prieditis and Flumerfelt, 1988). Bubbles in these trains can be quite large (Falls et al., 1989), indicating that few of the throats along the paths are blocked, while the fraction of throats blocked in the trapped gas region is presumably large. In addition, the lamellae within the train take a variety of positions in the pore bodies and throats. Some lamellae, by virtue of their position, actually promote movement of the train (Prieditis and Flumerfelt, 1988). We treat the mobilization pressure gradient of flowing foams in a separate study (Rossen, 1990a, b, c).

Conclusions

1. The percolation theory described here explains experimental reports of a minimum pressure gradient or injection rate required to generate a foam. This theory focuses on the pressure gradient required to mobilize lenses present in steady flow and lamellae formed by snap-off during imbibition. The theory predicts that, for most foams, foam mobilization is likely only at the high pressure gradients found near wellbore. Deep foam penetration therefore depends on propagation of the foam formed near the well.

2. Lower surface tension makes mobilization of CO_2 foams possible at lower pressure gradients. Our model indicates that

relatively wet CO_2 foam can be mobilized at 45 kPa/m (2 psi/ft) or less. Thus, CO_2 foam mobilization well away from an injection well in field application appears feasible.

3. New experimental results show that the minimum velocity to generate a flowing foam during steady flow, v_g^{min}, decreases with increasing injected *LVF*. In other words, foam can be generated at lower injection velocity if *LVF* is higher.

4. The theory for initial foam mobilization correctly predicts how v_g^{min} depends on *LVF*. The predicted values of v_g^{min} were larger than observed in corefloods, however. Very limited data suggest that the theoretically predicted values of $(\nabla p)^{min}$ are about right.

5. The importance of snap-off to lamella creation and mobilization suggests that alternate injection of liquid and gas slugs is a superior foam-generation strategy to steady, simultaneous injection of liquid and gas. However, theory indicates that except for CO_2 foams, foam mobilization in the field requires that slugs contact each other in the near-wellbore region where ∇p is high enough to mobilize the lamellae formed.

Acknowledgment

The authors thank F. Friedmann and J. H. Bae for stimulating discussion of these topics and P. R. Gutierrez and H. Duran for performing the experimental work.

Notation

$B(f)$ = backbone fraction; fraction of pore throats occupied by gas and able to conduct gas flow
f = open fraction, parameter in percolation theory
f_c = percolation threshold; value of f where first infinite cluster is formed and gas flow begins
f^0 = initial value of f when surfactant is introduced
f_{sn} = fraction of throats once occupied by gas, later blocked by snap-off, Eq. 3
$F(f)$ = percolation fraction; fraction of pore throats occupied by gas and connected to the backbone fraction
F_{tr} = fraction of gas saturation that is trapped, Eq. 4
$G(f)$ = conductivity of a partially occupied network, normalized so $G(l) = 1$
k = absolute permeability
k_{rg} = relative permeability to gas
ℓ = length of a single pore
L = projected length of blocked pore pathway in direction of flow (continuous gas foam)
L' = average distance between lamellae in flow pathway (discontinuous gas foam)
LVF = injected liquid volume fraction
n = number of pores in a pore cluster prevented from joining backbone by one blocked pore throat
$\bar{n}$ = average value of n taken over all pore throats blocking such clusters
∇p = macroscopic average pressure gradient
$(\nabla p)^{min}$ = minimum value of ∇p to mobilize lenses and lamellae
$(\Delta p)^{max}$ = maximum static pressure difference across a lamella as it is displaced from pore throat; also the minimum Δp required to displace it fully from throat, Eq. 1
Δp_t = total pressure drop across core
P_c = capillary pressure
r_t = radius of circular pore throat
$\bar{r}_{min}$ = minimum value of $2(1/r_1 + 1/r_2)^{-1}$, where r_1 and r_2 are principal radii of curvature of a lamella as it is displaced from throat
RF = resistance factor, Eq. 12
$S(f)$ = average cluster size (number of bonds) for $f < f_c$, Eq. 10
v_g = gas frontal advance rate
v_g^{min} = minimum or critical value of gas frontal advance rate for foam mobilization, Eq. 8
Z = length of core
z = coordination number of Bethe tree

Greek letters

γ = gas–liquid surface tension
γ_B = exponent in scaling law for B near f_c
μ_g = gas viscosity
μ_w = water viscosity
ϕ = porosity

Literature Cited

Ali, J., R. W. Burley, and C. W. Smutt, "Foam Enhanced Oil Recovery from Sand Packs," *Chem. Eng. Res. Des.*, **63,** 101 (1985).

Baghdikian, S., and L. L. Handy, "Flow of Foaming Solutions in Porous Media," *Modification of Chemical and Physical Factors in Steamflood to Increase Heavy Oil Recovery*, Y. C. Yortsos, U. S. Dept. Energy Ann. Rep., DOE/BC/14126–14, Bartlesville, OK (Feb. 1990).

Bailey, R. E., and L. B. Curtis, *Enhanced Oil Recovery*, Nat. Petroleum Council, Washington, DC (1984).

Bikerman, J. J., *Foams*, Springer, New York, 3, 67, 98–148 (1973).

Collins, R. E., *Flow of Fluids Through Porous Materials*, Reinhold, New York 144 (1961).

Coniglio, A., "Cluster Structure Near the Percolation Threshold," *J. Phys. A*, **15,** 3829 (1982).

de Arcangelis, L., S. Redner, and A. Coniglio, "Multiscaling Approach in Random Resistor and Random Superconductor Networks," *Phys. Rev. B*, **36,** 4656 (1986).

Duxbury, P. M., P. D. Beale, and P. L. Leath, "Size Effects of Electrical Breakdown in Quenched Random Media," *Phys. Rev. Lett.*, **57,** 1052 (1986).

———, "Breakdown Properties of Quenched Random Systems: The Random-Fuse Network," *Phys. Rev. B.*, **36,** 367 (1987).

Essam, J. W., "Percolation Theory," *Rep. Prog. Phys.*, **43,** 53 (1980).

Falls, A. H., G. J. Hirasaki, T. W. Patzek, P. A. Gauglitz, D. D. Miller, and J. Ratulowski, "Development of a Mechanistic Foam Simulator: The Population Balance and Generation by Snap-Off," *Soc. Petr. Eng. Reservoir Eng.*, **3,** 884 (1988).

Falls, A. H., J. J. Musters, and J. Ratulowski, "The Apparent Viscosity of Foams in Homogeneous Beadpacks," *Soc. Petr. Eng. Reservoir Eng.*, **4,** 155 (1989).

Fisher, M. E., and J. W. Essam, "Some Cluster Size and Percolation Problems," *J. Math. Phys.*, **2,** 609 (1961).

Flory, P. J., *Principles of Polymer Chemistry*, Cornell Univ. Press, Ithaca, NY, 402 ff. (1953).

Friedmann, F., and J. A. Jensen, "Some Parameters Influencing the Formation and Propagation of Foams in Porous Media," SPE 15087, Calif. Reg. Meet., Soc. Petr. Eng. (1986).

Friedmann, F., W. H. Chen, and P. A. Gauglitz, "Experimental and Simulation Study of High-Temperature Foam Displacement in Porous Media," SPE 17357, Soc. Petr. Eng./DOE Symp. on Enhanced Oil Recovery, Tulsa (1988).

Heiba, A. A., M. Sahimi, L. E. Scriven, and H. T. Davis, "Percolation Theory of Two-Phase Relative Permeability," SPE 15087, Calif. Reg. Meet., Soc. Petr. Eng. (1982).

Heiba, A. A., H. T. Davis, and L. E. Scriven, "Statistical Network Theory of Three-Phase Relative Permeabilities," SPE 12690, Soc. Petr. Eng./DOE Symp. on Enhanced Oil Recovery, Tulsa, (1984).

Herrmann, H. J., and H. E. Stanley, "Building Blocks of Percolation Clusters: Volatile Fractals," *Phys. Rev. Lett.*, **53,** 1121 (1984).

Herrmann, H. J., D. C. Hong, and H. E. Stanley, "Backbone and Elastic Backbone of Percolation Clusters Obtained by the New Method of 'Burning'," *J. Phys. A*, **17,** L261 (1984).

Hirasaki, G. J., and J. B. Lawson, "Mechanisms of Foam Flow in Porous Media: Apparent Viscosity in Smooth Capillaries," *Soc. Petr. Eng. J.*, **25,** 176 (1985).

Huang, D. D., A. Nikolov, and D. T. Wasan, "Foams: Basic Properties with Application to Porous Media," *Langmuir*, **2,** 672 (1986).

Huh, D. G., and L. L. Handy, "Comparison of Steady- and Unsteady-State Flow of Gas and Foaming Solution in Porous Media, *Soc. Petr. Eng. Reservoir Eng.*, **4,** 77 (1989).

Huh, D. G., T. D. Cochrane, and F. S. Kovarik, "The Effect of Microscopic Heterogeneity of CO_2-Foam Mobility: 1: A Mechanistic Study," *J. Petr. Technol.*, **41,** 872 (1989).

Isaacs, E. E., G. C. McCarthy, and J. D. Maunde, "Investigation of Foam Stability in Porous Media at Elevated Temperatures," *Soc. Petr. Eng. Reservoir Eng.*, **3**, 565 (1988).
Jerauld, G. J., L. E. Scriven, and H. T. Davis, "Percolation and Conductance on the 3D Voronoi and Regular Networks: A Second Case Study in Topological Disorder," *J. Phys. C*, **17**, 3249 (1984).
Kahng, B., G. G. Batrouni, and S. Redner, "Logarithmic Anomalies in Random Resistor Networks," *J. Phys. A*, **20**, L827 (1987).
Katz, A. J., and A. H. Thompson, "Quantitative Prediction of Permeability in Porous Rock," *Phys. Rev. B*, **34**, 8179 (1986).
Khatib, Z. I., G. J. Hirasaki, and A. H. Falls, "Effects of Capillary Pressure on Coalescence and Phase Mobilities in Foams Flowing Through Porous Media," *Soc. Petr. Eng. Reservoir Eng.*, **3**, 919 (1988).
Kirkpatrick, S., "The Geometry of the Percolation Threshold," *Electrical Transport and Optical Properties of Inhomogenous Media*, J. C. Garland, D. B. Tanner, eds., Am. Inst. Phys., New York (1978).
Larson, R. G., and H. T. Davis, "Conducting Backbone in Percolating Bethe Lattices," *J. Phys. C*, **15**, 2327 (1982).
Larson, R. G., and N. R. Morrow, "Effect of Sample Size on Capillary Pressures in Porous Media," *Powder Technol.*, **30**, 123 (1981).
Larson, R. G., L. E. Scriven, and H. T. Davis, "Percolation Theory of Residual Phases in Porous Media," *Nature*, **268**, 409 (1977).
———, "Displacement of Residual Non-Wetting Phases from Porous Media," *Chem. Eng. Sci.*, **36**, 75 (1981a).
———, "Percolation Theory of Two-Phase Flow in Porous Media," *Chem. Eng. Sci.*, **36**, 57 (1981b).
Lau, H. C., and S. M. O'Brien, "Effects of Spreading and Nonspreading Oils on Foam Propagation Through Porous Media," *Soc. Petr. Eng. Reservoir Eng.*, **3**, 893 (1988).
Lenormand, R., C. Zarcone, and A. Sarr, "Mechanics of the Displacement of One Fluid by Another in a Network of Capillary Ducts," *J. Fluid Mech.*, **135**, 337 (1983).
Mast, R. F., "Microscopic Behavior of Foam in Porous Media," SPE 3997, Soc. Petr. Eng. Ann. Meet. (1972).
Mohanty, K. K., J. M. Ottino, and H. T. Davis, "Reaction and Transport in Disordered Composite Media: Introduction of Percolation Concepts," *Chem. Eng. Sci.*, **37**, 905 (1982).
Owete, O. S., and W. E. Brigham, "Flow Behavior of Foam: A Porous Micromodel Study," *Soc. Petr. Eng. Reservoir Eng.* **2**, 315 (1987). (What is called the "pore neck" here is the short side of a narrow, wide trapezoid.)
Perry, R. H., and C. H. Chilton, eds., *Chemical Engineers Handbook*, 5th ed., McGraw-Hill, New York, 3-211 ff. (1973).
Pike, R. L., and H. E. Stanley, "Order Propagation Near the Percolation Threshold," *J. Phys. A*, **14** L169 (1981).
Prieditis, J., "A Pore Level Investigation of Foam Flow Behavior in Porous Media," Ph.D. Diss. Univ. Houston (1988).
Prieditis, J., and R. W. Flumerfelt, "Mobility of Foam in Porous Media," *Surfactant-Based Mobility Control: Progress in Miscible-Flood Enhanced Oil Recovery*, D. H. Smith, ed., *Am. Chem. Soc. Symp. Ser.*, **373**, Washington, DC (1988).
Ransohoff, T. C., and C. J. Radke, "Mechanics of Foam Generation in Glass Bead Packs," *Soc. Petr. Eng. Reservoir Eng.*, **3**, 573 (1988).
Ransohoff, T. C., P. A. Gauglitz and C. J. Radke, "Snap-Off of Gas Bubbles in Constricted Noncircular Capillaries," *AIChE J.*, **33**, 753 (1987).
Raza, S. H., "Plugging Formations with Foam," US Patent 3,491,832 (1970).
Roof, J. G., "Snap-Off of Oil Droplets in Water-Wet Pores," *Soc. Petr. Eng. J.*, **10**, 85 (1970).
Rossen, W. R., "A New Percolation Statistic With Unusual Properties," *J. Phys. A*, **21**, L533 (1988a).
———, "Theories of Foam Mobilization Pressure Gradient," SPE 17358, Soc. Petr. Eng./DOE Symp. on Enhanced Oil Recovery, Tulsa (1988b).
———, "Theory of Mobilization Pressure Gradient of Flowing Foams in Porous Media. I: Incompressible Foam," *J. Colloid Interf. Sci.*, **136**, 1 (1990a).
———, "Theory of Mobilization Pressure Gradient of Flowing Foams in Porous Media. II: Effect of Compressibility," *J. Colloid Interf. Sci.*, **136**, 17 (1990b).
———, "Theory of Mobilization Pressure Gradient of Flowing Foams in Porous Media. III: Asymmetric Lamella Shapes," *J. Colloid Interf. Sci.*, **136**, 38 (1990c).
Sanchez, J. M., and R. D. Hazlett, "Foam Flow Through an Oil-Wet Porous Medium: A Laboratory Study," SPE 19687, Soc. Pet. Eng. Ann. Meet. (1989).
Sanchez, J. M., R. S. Schecter, and A. Monsalve, "The Effect of Trace Quantities of Surfactant on Nitrogen/Water Relative Permeabilities," SPE 15446, Soc. Petr. Eng. Ann. Meet. (1986).
Sarychev, A. K., A. P. Vinogradoff, and A. M. Karimov, "Calculation of Percolation Conductivity in 3D," *J. Phys. C*, **18**, L105 (1985).
Sayegh, S. G., and M. Girard, "The Mobility of Carbon Dioxide Foams in Porous Media," Rept. 1988-2, Petroleum Recovery Inst., Calgary (Mar. 1988).
Slattery, J. C., "Interfacial Effects in the Displacement of Residual Oil by Foam," *AIChE J.*, **25**, 283 (1979).
Stanley, H. E., and A. Coniglio, "Fractal Structure of the Incipient Infinite Cluster in Percolation," *Percolation Structures and Processes*, G. Deutscher, R. Zallen, J. Adler, Eds., Israel Phys. Soc. (1983).
Stauffer, D., *Introduction to Percolation Theory*, Taylor and Francis, London (1985).
Stinchcombe, R. B., "The Branching Model for Percolation Theory and Electical Conductivity," *J. Phys. C*, **6**, L1 (1973).
———, "Conductivity and Spin-Wave Stiffness in Disordered Systems—An Exactly Soluble Model," *J. Phys. C*, **7**, 179 (1974).
Straley, J P., "Random Resistor Tree in an Applied Field," *J. Phys. C*, **10**, 3009 (1977).
Wardlaw, N. C., "Oil Recovery Efficiency and the Rock-Pore Properties of Some Sandstone Reservoirs," *Bull. Can. Petro. Geol.*, **27**, 117 (1979).
Wardlaw, N. C., and J. P. Cassan, "Estimation of Recovery Efficiency by Visual Observation of Pore Systems in Reservoir Rocks," *Bull. Can. Petro. Geol.*, **26**, 572 (1978).
Wellington, S. L., and H. J. Vinegar, "X-Ray Computerized Tomography," *J. Petr. Technol.*, **39**, 885 (1987).

Appendix: Refinements to the Model

A complete network theory of foam mobilization should begin with the realistic representation of the pore network, including realistic distributions of pore-throat radii and pore sizes (volumes). The pressure drops across individual lamellae would have to be determined by Monte Carlo studies on appropriate lattices. In addition, a complete study should account for gas invasion of liquid-filled pores as gas relative permeability drops and for the additional lamellae created by snap-off and leave-behind mechanisms during this invasion (Ransohoff and Radke, 1988). Even without surfactant, gas invasion is a complex percolation problem, a mixture of bond and site percolation. Gas entry into pores is governed by the pore throats, as in bond percolation, but in the absence of surfactant, liquid lenses between adjacent gas-occupied pores can thin down and break, as in site percolation.

The following are qualitative estimates of the effects expected were these refinements introduced.

Tortuosity and nonuniformity of ∇p

Recent numerical studies show that, near the percolation threshold f_c, conductivity depends on the relatively few links that join multiply connected blobs of open bonds (Pike and Stanley, 1981; Coniglio, 1982; Stanley and Coniglio, 1983). In contradiction to Eq. 2, the pressure gradient is not uniform under these conditions: most of the pressure drop occurs at the links, which can be short as one bond long (Duxbury et al., 1986, 1987; de Arcangelis et al., 1986; Kahng et al., 1987). As a result, near above the percolation threshold, the pressure drop can be large across clusters of only a few bonds. It is as yet unknown how near to f_c Eq. 2 can be used with reasonable accuracy. Certainly, very near f_c the minimum mobilization pressure gradient is less than that estimated here because the distance across which

significant pressure drops occur can be less than that indicated in Eq. 2. Further work is needed to quantify the error.

Substituting realistic three-dimensional networks for the Bethe tree, however, would increase the estimate of the mobilization pressure gradient in two ways. First, for continuous gas foams the product $f_c\gamma_B$, which controls $\bar{n}$, Eq. 6, is smaller for three-dimensional lattices than for the Bethe tree used here, Table 1. Second, for both continuous and discontinuous gas foams in three-dimensional networks, clusters become increasingly tortuous as their sizes increase near f_c. In the section Relating Average Cluster Size to $\triangle P$, we gave the approximation $L = (3\bar{n})^{1/2}\ell/2$ for the length of tortuous clusters. This length is less than assumed by Eq. 7, and the mobilization pressure gradient for tortuous clusters is greater. Although the exact relation for cluster lengths is unknown, tortuosity affects only the quantitative results; the qualitative conclusions do not change.

Nonuniform pores

Our theory assumes uniform pore conductivity but makes no assumption about pore size. Nonuniformity of pore size in real porous media means that occupied pore fractions cannot be equated with volumetric saturation. Nonuniformity of pore *conductances* introduces additional complications. In a real porous medium, gas invades the largest pore throats, with the highest conductances first. Thus, for a given liquid fractional flow, LVF, f^0 may be lower than that derived above and closer to the percolation threshold f_c. This suggests that a given fraction of throats blocked by snap-off would have greater effect than estimated here. The effect would be greatest in rocks with broad distributions of pore sizes. The work of Katz and Thompson (1986) suggests that in many rocks flow conductance varies by orders of magnitude among pores. However, the pore throats most likely to be blocked by snap-off are the smallest ones occupied by gas, which contribute least to gas flow. This, in contrast, suggests that for given f^0, a given reduction in gas flow would require a greater fraction of throats blocked than estimated here. Thus, the combined effects of nonuniform pores is difficult to predict a priori.

Actually, our model implicitly assumes that the pore-throat radii are not uniform. Otherwise, when the first lamella out of many was mobilized it would flow forever, blocking additional channels, reducing f, and thereby helping mobilize other lamellae. Instead we use a rather large estimate of the characteristic throat radius, 50 μm, and assume that the first few lamellae mobilized from throats with larger radius become stuck at the next throats, which are likely to be smaller. This allows us to disregard a finite fraction of the largest clusters and focus on those with $n = 3\bar{n}$.

Recent experimental results (Friedmann, unpublished results, 1988) suggest that the minimum velocity for foam generation is a function of surfactant type and concentration—factors known to affect coalescence (Bikerman, 1973; Huang et al., 1986; Khatib et al., 1988). None of the mechanisms for generation and mobilization described in this study should depend on these factors. Thus, it appears that observed foam "generation" in corefloods is in reality lamella generation and mobilization in sufficient quantity to overcome coalescence processes. If so, then the fraction of lamellae that must be mobilized, represented by $n \geq 3\bar{n}$ here, may be a function of surfactant type and concentration as well as other factors that affect coalescence.

$(\triangle p)^{max}$ a function of f

In our theory we use a fixed, rather low estimate of $(\triangle p)^{max}$, the microscopic $\triangle p$ required to mobilize the first lenses or lamellae. In a real porous medium, $(\triangle p)^{max}$ depends of f and on sample history.

Let r_t^0 correspond to the pore throat just enterable at the prevailing capillary pressure during drainage, p_c^0; that is, the throat for which

$$r_t^0 = 2\gamma/p_c^0 \tag{A1}$$

Decreasing LVF implies increasing p_c^0 and decreasing r_t^0. During drainage, in the absence of surfactant, all accessible throats with $r_t > r_t^0$ are invaded by gas, and if f is well above the percolation threshold, then virtually all throats are accessible. Additional, narrower throats are invaded by gas if the lenses between gas-occupied pores drain and break. When surfactant is introduced, the lenses available for mobilization have $r_t < r_t^0$, which depends on injected LVF during drainage. Thus $(\triangle p)^{max}$ is larger for smaller values of LVF in steady flow. Upon substantial subsequent imbibition, however, lenses and lamellae may form in pore throats with $r_t > r_t^0$, and these throats, with lower $(\triangle p)^{max}$, are the likely sites of initial mobilization. Thus $(\triangle p)^{max}$ for the sample as a whole depends both on initial injected LVF during drainage and on subsequent sample history.

Foam mobilization during drainage

The ease of mobilizing foam formed by drainage in the presence of surfactant depends on whether snap-off occurs and on the stability of lamellae formed by leave-behind. Our theory cannot address this process directly because the positions of lamellae in any case are far from random and uncorrelated. Here we make some qualitative observations.

If the lamellae formed by leave-behind do not break, then almost all the gas is dead-end, because none of the gas fingers can rejoin the backbone without rupturing such a lamella. In this case the clusters blocked by these lamellae could grow quite large and foam mobilization could be easy. This could explain why Ransohoff and Radke (1988) saw foam mobilization immediately as gas invaded the interior of a liquid-saturated beadpack. If so, then their results reflect primarily mobilization of leave-behind lamellae, not creation of new lamellae by snap-off as they hypothesized, although they did observe lamella generation by snap-off concurrent with mobilization.

If, on the other hand, lamellae formed by leave-behind rupture, then foam mobilization would not be as easy. Still, one cannot analyze the process with our theory because, during drainage, lamellae form by snap-off near the tips of invading gas fingers (Ransohoff et al., 1987), not randomly in space.

Similar arguments apply to imbibition, if snap-off blocks gas flow and as a result gas saturation subsequently rises to maintain constant fractional flow. As gas saturation rises, new lamellae are created by leave-behind. If the rise in gas saturation were substantial, it is possible that some of these dead-end clusters created could become large and lamellae could be mobilized at lower ∇p than estimated here.

Manuscript received Nov. 7, 1989, and revision received May 24, 1990.